NAIC-ID(RS)T-0389-94

NATIONAL AIR INTELLIGENCE CENTER

AIR INTELLIGENCE AGENCY

PHOTOREFRACTIVE $Bi_{12}SiO_{20}$ SPACIAL LIGHT MODULATOR

by

Zhao Mingjun, Li Yulin, Wang Zhao

NATIONAL AIR INTELLIGENCE CENTER

NAIC- ID(RS)T-0389-94

HUMAN TRANSLATION

NAIC-ID(RS)T-0389-94 29 December 1994

MICROFICHE NR: 95C000020

PHOTOREFRACTIVE $Bi_{12}SiO_{20}$ SPACIAL LIGHT MODULATOR

By: Zhao Mingjun, Li Yulin, Wang Zhao

English pages: 8

Source: Guangxue Xuebao, Vol. 11, Nr. 9, September 1991; pp. 810-814

Country of origin: China
Translated by: Leo Kanner Associates
F33657-88-D-2188
Quality Control: Ruth A. Peterson
Requester: NAIC/TATE/Capt Joe Romero
Approved for public release; Distribution unlimited.

THIS TRANSLATION IS A RENDITION OF THE ORIGINAL FOREIGN TEXT WITHOUT ANY ANALYTICAL OR EDITORIAL COMMENT STATEMENTS OR THEORIES ADVOCATED OR IMPLIED ARE THOSE OF THE SOURCE AND DO NOT NECESSARILY REFLECT THE POSITION OR OPINION OF THE NATIONAL AIR INTELLIGENCE CENTER.	PREPARED BY: TRANSLATION SERVICES NATIONAL AIR INTELLIGENCE CENTER WPAFB, OHIO

GRAPHICS DISCLAIMER

All figures, graphics, tables, equations, etc. merged into this translation were extracted from the best quality copy available.

PHOTOREFRACTIVE $Bi_{12}SiO_{20}$ SPACIAL LIGHT MODULATOR

AUTHORS: Zhao Mingjun, Li Yulin and Wang Zhao

Xian Institute of Optics and Precision Mechanics, Academia Sinica
Xian 710068

Received 8 November 1990, revised 5 February 1991

We used home-made photorefractive crystal $Bi_{12}SiO_{20}$ as a real-time non-degenerate and degenerate four-wave mixing medium to accomplish conversion from incoherent to coherent, wave length conversion, and image subtraction between coherent and incoherent image. The experimental results are presented in this paper.

I: INTRODUCTION

Devices or equipment which can modulate the spacial information of light, including amplitude, polarization, phase and even wave length are universally called spacial light modulators. This operation is determined by a type of distributed light information, called light addressing spacial light modulators. In light information processing and light computing systems,it is possible to use high speed, parallel processing and highly interconnected capabilities. Therefore, these are attracting more and more attention. Currently the more widely used spacial light modulators include the liquid crystal light valve, the variable reflective lens, the microchannel board spacial light modulator, the semiconductor multi-quantum trap, and magnetic optical devices[1,2]. The first to use optical refractive crystal $Bi_{12}SiO_{20}$

as a spacial light modulator was the PROM device (Pockels readout optical modulator)[3]. Later, on the basis of research on the non-linear effects of light refraction, Shi et al[4] proposed using optical refractive crystal four wave frequency and mixing adding non-coherent light modulation to achieve conversion of non-coherent images into coherent images, which is the PICOC (photorefractive incoherent-to-coherent optical converter). This adds something new to spacial light modulator development and application research[5].

On the basis of the authors' testing and research of the light refractive properties of China produced BSO crystals[6], this article reports for the first time its degenerative and non-degenerative multiple wave frequency mixing, achieving incoherent-to-coherent image conversion, and further using this system to achieve image storage, wave length conversion and coherent and incoherent image parallel image subtraction and presents the results of our experiments.

II: PHOTOREFRACTIVITY EFFECT AND FOUR WAVE FREQUENCY MIXING CONVERSION OPERATIONS

Fig. 1: Schematic diagram of photorefractive four wave mixing

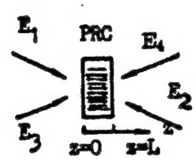

Figure 1 is a schematic diagram of photorefractive crystal four wave frequency mixing. Here, the pump wave E_1 and the signal wave E_3 form a cyclical strong light distribution inside the photorefractive crystal. The photocarriers produced by illumination shift from light areas to dark areas (diffusion and drift) and then set up spacial charged fields:

$$E_{sc}=E_q\left[\frac{E_a^2+E_d^2}{E_a^2+(E_d+E_q)^2}\right]^{1/2}, \tag{1}$$

Here, E_q is the largest charged field. E_d is the diffusion field. E_G is the applied electric field. The cyclical electrical field undergoes the electro-optic effect to modulate the crystal's refractivity, forming a cyclical distribution.

$$\Delta n = (1/2) n_b^3 r_{eff} E_{sc} \qquad (2)$$

In this equation, n_b is the refractivity of the crystal, is the effective electro-optical coefficient. Its photorefraction effect process is shown in Figure 2.

Fig. 2: Photorefractive effect process

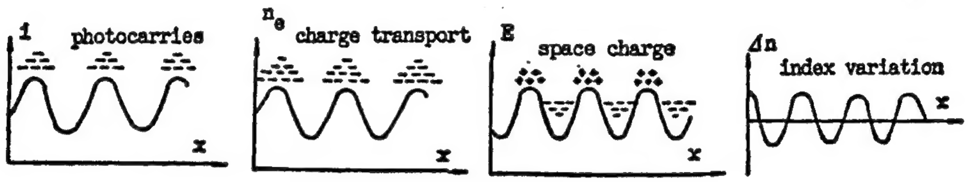

If we use the E^1 opposite, the pump wave E_2, as the read out wave, then we obtain E_3's complex conjugate wave E_4. This constitutes the so-called four frequency mixing system.

If in equation (1), $E_G > E_d$, and $E_q > E_G$, that is, the applied electrical field is the main conductor, then . Therefore, the change in the refractivity index is directly proportional to the applied electric field. For a further discussion of photorefractive BSO crystal phase conjugate and holographic optical gate diffraction see bibliographic item [6].

BSO crystals are cubic cells, point group 23. They have a marked electro-optical effect and conductive effect. Response time is three levels of magnitude faster than $BaTiO_3$ and $LiNbO_3$ crystals[7,8]. Figure 3 shows photorefractive BSO crystal ($10X10X3mm^3$) multiwave mixing to carry out incoherent-to-coherent optical conversion. The applied electric field (along axis 001) is parallel to the grating vector. If we use E_1 and E_3 to form an incoherent light or white light image on the crystal, this

incoherent light will form a grating with E_1 and E_3 which perform spacial modulation, and the post-modulation results will load the information carried on the incoherent light onto the spacial grating. If at the same time a coherent pump wave E_2 read out grating is used, then the output fourth conjugate wave will carry the incoherent light information. Thus completing the incoherent image to coherent image conversion.

Fig. 3: Experimental setup for PICOC in FWM with BSO crystal

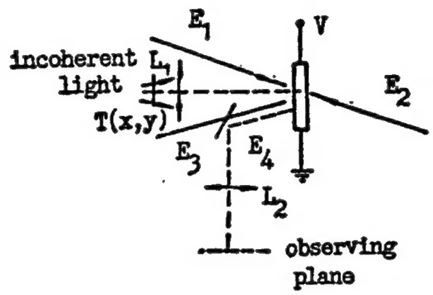

In the experiments used in this article, the four wave mixing used Ar+ laser light as the coherent light source (wave length of 514.5nm). The incoherent image used a white candescent bulb or fluorescent bulb light source passing through lens L_1(focal length of 22 cm, diameter of 5 cm) to form an image on the BSO crystal. On the crystal we applied a high voltage electric field of $8kv \cdot cm^{-1}$. Figure 4 shows the results of the conversion.

Fig. 4: The results of the PICOC operation

(a) (b)

(a). Input of an incoherent image. (b). Output of a negative replica of the input image.

Figure 5(a) shows the use of non-degenerative multiple wave mixing to accomplish PICOC operations. The I_1 and I_2 from the laser (514.5 nm) have an effect on the external field,and establish a

bulk grating on the BSO. Another He-Ne laser light (632.8 nm) satisfies the Braggs condition, and is directed at the BSO, diffracting the fourth beam of He-Ne light. If I_1 and I_2 include spacial information, or if their incoherent information is modulated onto a grating, then it can be transmitted the He-Ne light being diffracted out as shown in Figure 5(b). Here, T(x,y) is incoherent information. In Figure 5(b) T(x,y) is spacial image information in I_2 light.

Fig. 5: PICOC performed by using real-time holography.

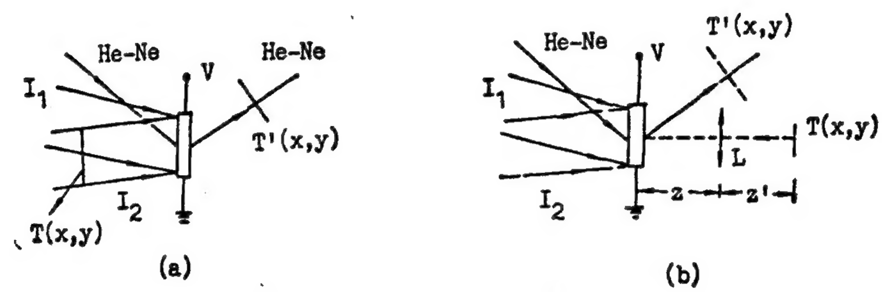

(a). Green image (514.5 nm) was stored, it can be readout by red light (632.8 nm). (b). White image was stored, it can be readout by red (632.8 nm) or green (514.5 nm) light.

III: EXAMPLES OF IMAGE PROCESSING

A number of reports have already been published concerning the use of photorefractive BSO crystal multiwave missing to achieve image processing[9,10]. However, these have all concerned pure coherent computations. Here, based on the foregoing theories, the authors have used these in image processing including incoherent and coherent images as well as optical calculation operations.

1. IMAGE STORING AND WAVE LENGTH CONVERSION

Fig 6. The curve of diffraction efficiency dependence time for grating build up and decay in BSO (10X10X3 mm3); E_a=ykV·cm^{-1}) crystal[6]

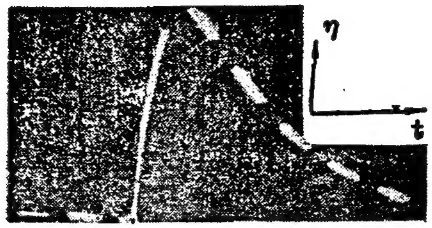

Because BSO crystals have live time recording and storing capabilities, and more importantly, when there is an applied electrical field, they have a rapid grating establishing speed and a slow degeneration process[6]. As Figure 6 shows, when I_1 and I_2 are used to expose the crystal, and then using a white light image to focus on the crystal, it generally takes a fair amount of time (0.1 to 1 second). This is primarily determined by the intensity of the white light, the greater the intensity, the shorter the exposure time. At this time, the light from the Ar+ laser can be cut off, freezing the incoherent image inside the crystal. After a few minutes, if a plane wave of He-Ne or Ar+ light (I_1 or I_2) is used to read the grating, a coherent red light or green light image can be obtained. This completes the transformation of white light into red light (632.8nm) or green light (514.5nm) wave length image as shown in Figure 7. During the process of building up an I_1 and I_2 grate, because of the characteristic local response of the BSO crystal, if the I_1 or I_2 itself contains spacial information, and a transparent object is placed into the I_1 or I_2 optical circuit, then using the He-Ne light to read it out, it is possible to obtain the corresponding spacial image as shown in Figure 8, thus completing the wave length transformation of a green light (514.5nm) image into a red light (632.8nm) image (this is a positive image transformation).

Fig. 7: Image conversion corresponding with Fig. 5(B)

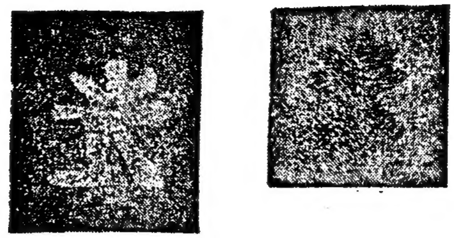

(a) (b)

(a). White light image (input). (b). Red or green image (output).

Fig. 8: Image conversion from green image (514.5nm) to red image (632.8nm) corresponding to Fig. 5(1).

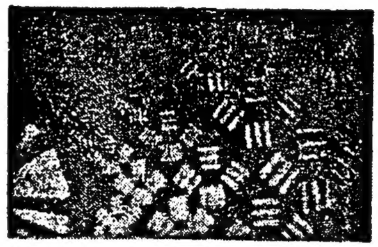

2. PARALLEL IMAGE SUBTRACTION OPERATION OF INCOHERENT AND COHERENT IMAGE

Fig. 9: Parallel image subtraction between coherent and incoherent images

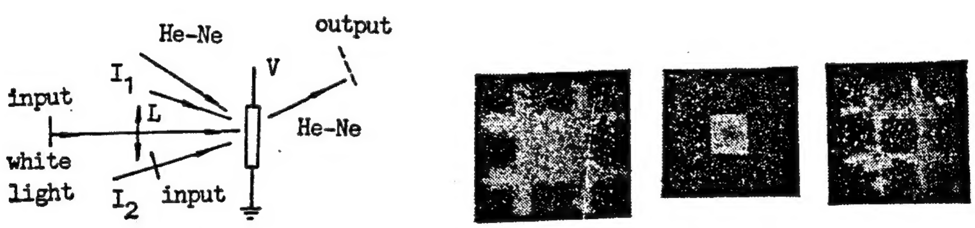

(a) (b) (c) (d)

(a). Diagram of image subtraction by FWM and white light writing. (b).Coherent image for I_2 path inputting. (c). Coherent image for white light image inputting. (d). The resultant output of subtraction between (b) and (c).

In the conversion process described above from incoherent to coherent images, the operational result is the negative of a white light image. This is due to the fact that the white light image written in serves to remove inherent grating, so from the writing

in to the reading out of the white light image is about the same thing as "negative" computation, while the coherent light I_1 (or I_2) is written in positive. If one of the coherent lights (I_1 or I_2) and the incoherent lights each carry an image, this operation is the equivalent of parallel image subtraction between the two, and the computational results can be read out using the He-Ne light as shown in Figure 9. Similarly, this method can be applied to photologic operational computations.

In summary, this type of spacial light modulator is simple in structure, can be used repeatedly, has high speed reaction, live time operation, and at the same time does not effect the crystal being reused for non-linear optical and live time holograms. This fills in an important portion for practical research into photorefractive crystals in spacial optical modulators and optical computing.

Mister Xu Liangying of the Shanghai Silicate Laboratory provided some of the crystals used in our experiments. Intern Yao Lixin of the Beijing Industrial University participated in some of the work of our experiments. Zhu Xilao, Kong Yu'e and Yao Li of the Xian Institute of Optics and Precision Mechanics were a great help. We take this opportunity to express our gratitude to these individuals.

BIBLIOGRAPHY

[1] D. Casasent; *Opt. Engng*, 1978, **17**, No. 4 (Jul/Aug), 307.
[2] Spatcal Light Modulations & Applications 1988.
[3] R. A. Sprague, P. Nisenson; *Opt. Engng*, 1978, **17**, No. 4 (Jul/Aug). **256.**
[4] Y. Shi, D. Psaltis *et al.*; *Appl. Opt.*, 1983, **22**, No. 23 (Dec), 3665.
[5] Scapham, R. W. Eason *et al.*; *Opt. Commun*, 1990, **74**, No. 5, 290.
[6] Li Yulin, Zhao Mingjun; *Proc. SPIE*, 1990, Vol. 1358
[7] W. J. Burke, D. L. Staebler *et al.*; *Opt. Engng*, 1978, **17**, No. 4 (Jul/Aug). **308.**

DISTRIBUTION LIST

DISTRIBUTION DIRECT TO RECIPIENT

ORGANIZATION	MICROFICHE
B085 DIA/RTS-2FI	1
C509 BALLOC509 BALLISTIC RES LAB	1
C510 R&T LABS/AVEADCOM	1
C513 ARRADCOM	1
C535 AVRADCOM/TSARCOM	1
C539 TRASANA	1
Q592 FSTC	4
Q619 MSIC REDSTONE	1
Q008 NTIC	1
Q043 AFMIC-IS	1
E051 HQ USAF/INET	1
E404 AEDC/DOF	1
E408 AFWL	1
E410 AFDTC/IN	1
E429 SD/IND	1
P005 DOE/ISA/DDI	1
P050 CIA/OCR/ADD/SD	2
1051 AFIT/LDE	1
P090 NSA/CDB	1
2206 FSL	1

Microfiche Nbr: FTD95C000020I
NAIC-ID(RS)T-0389-94